Acta Scientific Applied Physics

Volume 3 Issue 6 June 2023

Research Article

Imaging of Antiferromagnetic Domains by Using Magneto-Optical Birefringence Effect Microscopy Technique: An Overview

Sucheta Mondal*

Department of Physics, School of Natural Sciences, Shiv Nadar Institution of Eminence, Tehsil Dadri, Gautam Buddha Nagar, Uttar Pradesh, India

***Corresponding Author:** Sucheta Mondal, Department of Physics, School of Natural Sciences, Shiv Nadar Institution of Eminence, Tehsil Dadri, Gautam Buddha Nagar, Uttar Pradesh, India.

Received: May 17, 2023;

Published: May 31, 2023

Abstract

The emerging field of 'Antiferromagnetic Spintronics' is one of the most promising contenders for the next-generation information storage and processing applications. Antiferromagnets are immune to the external magnetic field of magnitude up to few Tesla! They have high exchange anisotropy and zero dipolar field. These characteristics promote them as suitable candidates for designing denser, faster, and energy-efficient spintronic devices. To integrate antiferromagnetic components inside an on-chip microelectronic circuitry it is important to manipulate the magnetic states with small charge current. However, when it comes to the detection, zero dipole moment makes them irresponsive to the conventional magnetometry measurements. It requires probing with state-of-the- art facilities which is not accessible to everyone. Thus, it is difficult to establish the connection between the electric current driven spin-transport behavior and the domain modification without capturing the inside picture simultaneously. In this mini-review, a brief history of antiferromagnetic switching and the recent conflicts on the all-electrical manipulation of Neel vector are discussed. This is followed by an overview of the magneto-optical birefringence effect microscopy technique and its implementation for validating electrical switching with optical imaging. This article aims to provide the readers a broader idea about an unambiguous and powerful technique to visualize the enigmatic antiferromagnetic domains on the table top of a laboratory.

Keywords: Antiferromagnet; Magneto-optical Birefringence Effect; Neel Vector; Polarization; Anisotropy; Antiferromagnetic Switching

Abbreviations

AFM: Antiferromagnet; SOT: Spin-orbit Torque; MOBE: Magneto-Optical Birefringence Microscopy; AMR: Anisotropic Magneto Resistance; AHE: Anomalous Hall Effect; SHE: Spin Hall Effect; XMLD: X-ray Magnetic Linear Dichroism; PEEM: Photoemission Electron Microscopy;

Introduction

Absence of enough evidences for electrical switching in the antiferromagnetic (AFM) devices unfurled huge debate amongst the scientists who have been working on such systems for the last few decades. In 2019, Chiang., *et al*. reported a recurring change in the magnetoresistance signal within the nonmagnetic devices that showed uncanny resemblance with multi-level switching like behavior previously observed in the AFM heterostructures [1]. The signal strength obtained from such devices consisting of only nonmagnetic metal found to be higher than the devices with AFM layers. They claimed that the signal originates from the thermal response of the metallic lattice due to application of current pulses which does not have any magnetic origin. It confronts the popular all-electrical methods for detecting the Neel-vector switching in AFM heterostructures!

At this point, a brief history of AFM switching will help the reader to understand the literal context of this debate. Louis Neel

received the Noble Prize in 1970 for his seminal work on the AFMs. Though he himself addressed AFMs as 'interesting but useless', the quest for exploring exquisite properties of the two-dimensional and three- dimensional systems with AFM ordering has never been stopped. Despite of not having a furious start in the application front, the emerging field of AFM spintronics is one of the contenders for the next-generation information storage and processing technology [2]. The antiparallel alignment of the spins within an AFM lattice results in zero magnetic moment as well as zero dipolar field. This further makes them inert to the external magnetic-field of Tesla order and allows a multilevel stability in the memory devices eliminating the problem of 'cross-talking' [3]. The spin dynamics with THz frequency observed for the AFMs is a consequence of their high exchange anisotropy which will be beneficial for designing ultrahigh-speed data processing applications [4]. The spin-flop field for most of the AFMs are unrealistically high which is advantageous for construction of nonvolatile memory components as such a high field strength is not accessible in our day-to-day life. In one hand it makes the AFM devices robust to external perturbation and keeps the information secured. On the other hand, it causes difficulty in data-writing. Thus, it is very important to look for alternatives in order to switch the Neel vector other than assistance from magnetic field. Exploitation of charge current could be a sustainable approach in such cases where AFMs are supposed to be integrated within on-chip circuitry and must be compatible with the current microelectronic technology. The electrical detection of the magnetization vector has been realized in several ways, such as, probing anisotropic magnetoresistance (AMR), [5] anomalous Hall effect (AHE), [6] spin Hall effect (SHE) [7] etc. However, the efficient means for altering the magnetic states have remained elusive until 2016 when Wadley., *et al*. discovered the electrical switching driven by an intrinsic spin- orbit torque (SOT) in metallic AFM, i.e., CuMnAs [8]. This Neel-order SOT originated from inverse-spin galvanic effect within the material itself was predicted in Mn2Au in 2014 [9] however the first experimental evidence was reported later in 2018 [5]. Eventually scientists have realized that thermal activation and thermal assistance via Joule heating can lead to the stability of multi-level states in the Mn-based AFM devices. The inverse spin-galvanic mechanism will generate locally non-equilibrium spin polarizations of opposite polarities on the inversion-partner of Mn sublattices. For these staggered fields to couple strongly to the AFM order it is essential criteria that the inversion-partner Mn sublattices coincide with the two spin-sublattices of the AFM ground-state. However, very few exotic metallic AFMs can exhibit such broken symmetry within the lattice itself which poses a sever challenge in the application front. Abundance and cost effectiveness of the raw material are the matters of concern in the industry level. It is also important to mention that in order to utilize the switching between two states of an AFM domain, the Neel vector must alter between two orthogonal easy axes. 180° switching observed in AFM systems might not be helpful as before and after switching, the effective magnitude and direction of Neel vector is unchanged and hence effectively unrecognizable as '0' or '1' without a passive detcetion.10 From the application point of view the hassle-free writing and reading process are also desirable while designing new device prototypes. Recently, SOT induced switching of insulating NiO is reported via the SHE of an adjacent Pt layer results in very similar switching characteristics as Mn2Au or CuMnAs [11-13]. While the details of the underlying mechanism are under debate, it nevertheless opens a new route in AFM spintronics. For heterostructures containing insulating AFMs, current should be sent through a nonmagnetic metallic layer adjacent to it. Electromigration and other thermal artifacts come into the picture when the current goes beyond the Ohmic regime in such multi-terminal devices. Electromigration occurs as the current density becomes high and the heat dissipated within the material breaks the atoms from the structure creating both 'vacancies' and 'deposits' at the microscopic level. It results in a recurring change in the resistance of the device exhibiting similar trend as multi-level magnetoresistance signal found in AFMs1 (see Figure 1). Thus, it is not recommended to rely solely on the all-electrical measurements to investigate real AFM switching!

A popular phrase, 'Seeing is believing', is indeed relevant here. It is extremely important to visualize the domain modification simultaneously with electrical switching in order to validate the authenticity of the results. Due to having compensated magnetic moments AFM domain contrast is very difficult to probe using any conventional magnetometries or spectroscopies as mentioned earlier. It demands probing with the state-of-the-art facilities. The very first experimental observation of AFM ordering was conducted by using neutron diffraction technique in 1950 [14]. Afterwards a bunch of microscopy techniques were exploited to capture AFM domains in different types of materials [15]. Spin-polarized scanning tunneling microscopy [16], scanning single-spin magnetometer [17], and magnetic exchange force microscopy18 etc. have been used for the

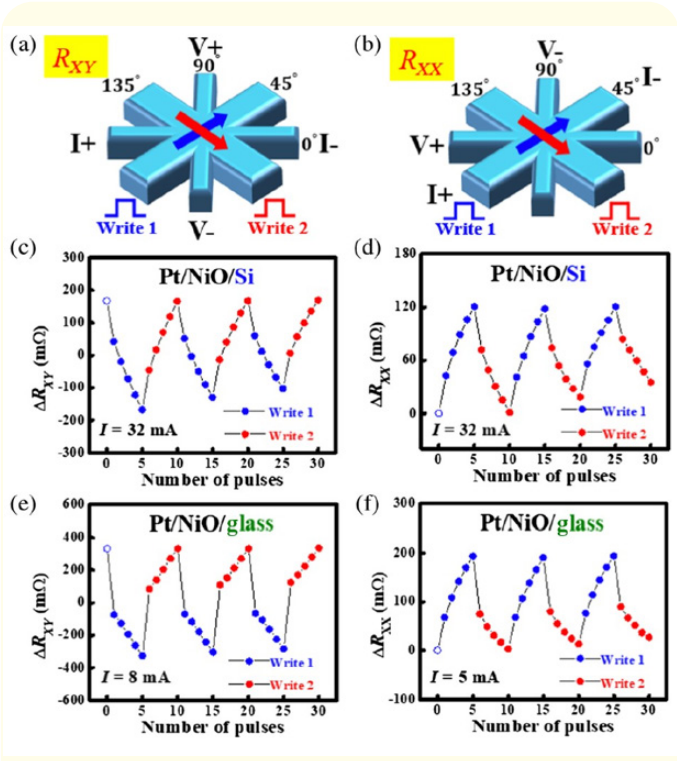

Figure 1: Schematics of the eight-terminal patterned structure with the pulsed writing current along the 45° (write 1) and the 135° (write 2) lines for (a) planar Hall and (b) longitudinal resistance measurements. Relative changes of Hall resistance (ΔR_{XY}) in (c) Pt/NiO/Si and (e) Pt/NiO/glass and relative change of longitudinal resistance (ΔR_{XX}) in (d) Pt/NiO/Si and (f) Pt/NiO/glass, after applying 10-ms writing current pulses alternately along the 45° and the 135° lines. Reproduced from Ref. 1 with permission from American Physical Society.

imaging since long back. However, these studies require ordered and pristine sample surfaces which can only be achieved by using high-end growth facilities which are expensive and not easily accessible. It is pertinent to mention here that X-ray magnetic linear dichroism (XMLD) based photoemission electron microscopy (PEEM) is the most popular technique that scientists have been using to visualize AFM domains [8,19,20]. However, to study current-induced domain modification one needs to incorporate magneto-transport measurement facilities with the PEEM instrument. Though researcher have invested their time and effort in doing so, this customization is not always straightforward in the beamline environment and requires special training. Magneto- optical Kerr effect (MOKE) technique [21] is one alternative to study magnetic activities within non-collinear AFMs with canted spin structures and finite magnetic moment [22]. However, till date this technique has not been sufficient to probe the Neel vector orientation within the collinear AFMs having compensated magnetic moment. Recently, Voigt effect-based femtosecond pump-probe technique is exploited for probing the dynamics in metallic CuMnAs [23]. It is important to mention here that the polarization rotation observed in Voigt effect depends on the quadratic form of sublattice magnetization. Thus, unlike the Kerr and the Faraday effects, it can be reliably used for capturing AFM domain contrasts. The terminology is not unique. It is also denoted as magnetic birefringence sometimes. Furthermore, in reflection geometry scientists call it quadratic MOKE and Hubert-Schäfer effect. If the intensity variation in transmitted or reflected geometry is recorded after the interaction of the light in parallel and perpendicular configuration to the magnetic moments, the name magnetic linear dichroism (MLD) is used.

While discussing switching in metallic AFMs, it is important to shed some lights on the popularity of insulating NiO as one of the most common and natural transition-metal oxides. This is an attractive candidate on which plethora of theoretical and experimental studies have been reported so far. It can exhibit 90° switching along the orthogonal easy axes which is desirable in many proposed magnetic applications. Not only the bulk NiO and the thin films but also exchange-coupled heterostructures consisting of NiO and ferromagnet have been subjected to domain imaging investigations [20,24,25]. Magneto- optical birefringence effect (MOBE) based imaging can be another suitable approach to visualize AFM domain contrasts in NiO. These contrasts arise due to the rhombohedral deformation in the lattice. The MOBE microscopy technique can be developed on the table top inside a laboratory. This is a cost-effective, easily accessible, and straight forward method in comparison to the other microscopies which are based on synchrotron facilities. There are also two close contenders of the MOBE technique, i.e. magnetic second harmonic generation (MSHG) microscopy [26] and Seebeck effect imaging [27] which can be implemented on the table top and can reliably capture AFM domains.

In this mini-review, the basic principle of the MOBE microscopy and some of the recent progresses are discussed highlighting the need for validation of electrical switching with simultaneous optical imaging of the AFM devices. This is followed by the scope of improvements and the future perspective. This article will help the reader to gain a broader idea about of this relatively unambiguous

and powerful optical microscopy technique to visualize the 'stubborn' AFM domains!

Overview of the MOBE microscopy technique

Previously MOBE microscopy technique has been used often in the transmission geometry and seldom in the reflection geometry [23,28,29]. MOBE signal is produced by the modification of refraction indices parallel ($n_{||}$) and perpendicular ($n_{\perp}$) to the magnetization vector (M). In a typical reflection geometry, if the incident light is linearly polarized and it has an offset ϕ with M, the reflected light experiences a small polarization rotation $\theta_{!}$, which can be expressed as follows,

$$\theta_{\upsilon} = \frac{r_{||}-r_{\perp}}{r_{||}+r_{\perp}} sin2\phi \quad \text{--------(1)}$$

Here $r_{||}$ and $r_{\perp}$ are the reflection coefficients for polarizations along parallel and perpendicular directions to the magnetization, respectively. This is due to having different response from the two different refractive indices. Thus, it is observed that optical contrasts can be achieved due to the opposite polarization rotation of the light reflected from the regions with orthogonal Neel vectors. This is a very effective method in order to distinguish and identify different AFM domains.

In 2019, Xu., *et al*. propose an experiment on NiO thin films grown on MgO substrate by using a Evico magneto-optical Kerr microscope [30]. This instrument is specially designed and consists of several optical components, such as, polarizers, analyzers, waveplates, mirrors, beam-splitters, microscope objective, charge-coupled device (CCD) camera and a white LED source. No magnetic field is applied during the experiment. The experimental geometry is presented in Figure 2(a). For the sake of the demonstration, they have considered two orthogonal AFM domains (say, domain A and B) within the field of view of the microscope. Now suppose, the light is incident with polarization 45° away from the projected component of the Neel vector of the NiO spins in the sample plane, θ_{υ} corresponding to domain A has opposite sign when that corresponds to domain B (θ_{υ} and $-\theta_{\upsilon}$). Now the analyzer is initially set to extinction position with the polarizer angle to eliminate any unwanted optical contrast from the sample surface. After rotating the analyzer by an angle θ from the extinction position the detector on the CCD surface can capture light with intensity (I). This is usually proportional to $\sin^2(\theta - \theta_{\upsilon})$ for domain A and $\sin^2(\theta + \theta_{\upsilon})$ for domain B which gives rise to desired optical contrast on the image.

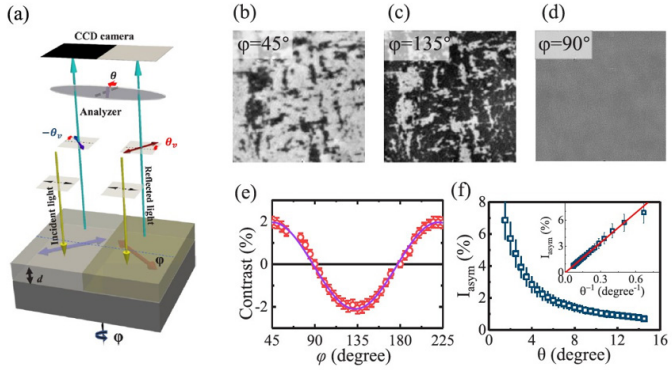

Figure 2: (a) Schematics of magneto-optical microscopy measurement geometry. (b–d) The typical domain images of a 20-nm-thick NiO Ñilm on MgO(100), obtained from the magneto-optical microscope at room temperature with ϕ = 45°, 135°, and 90°, respectively. The size for all the images is 40 x 40 μm^2. (e) The quantiÑied optical contrasts from the NiO domains as a function of ϕ. The purple line represents a Ñitting curve of sin2ϕ. (f) The optical signal symmetry as a function of θ; the inset demonstrates the linear dependence of Iasym as a function of θ−1. Reproduced from Ref. 30 with permission from American Physical Society.

However, in practice this contrast (dark and bright patches on the Figure 2 (b, c, d)) can be originated from nonmagnetic contributions from the surface morphology of the entire device (roughness, defects, patterning etc.), fragmented magnetic domains inside the AFM layer or both. Nonmagnetic contribution may appear due areas with just different reflection intensity without any polarization rotation. This response should be identified by rotating the analyzer angle to the opposite angle -θ which should result in the same contrast. Thus, if the signal asymmetry is obtained by performing the following treatment for the two optical images, the difference image will be free from any artifacts showing only the magnetic contrasts.

$$I_{asym} = \frac{I(+\theta)-I(-\theta)}{I(+\theta)+I(-\theta)} \quad \text{--------(2)}$$

nce of the intensities on the ϕ and the θ further confirms the magnetic origin (see Figure 2 (e, f)). In this study, the NiO (001) film has four-fold symmetry on the sample plane. Thus, only two types of contrasts are observed for the two orthogonal T-domains detectable using MOBE technique. The intensity asymmetry derived from a ϕ-dependent contrast agrees with

present literature in transmission geometry for other magnetic materials. It is interesting fact that observed polarization rotation for a 20-nm-thick NiO film is 60 mdeg which is undoubtedly larger than the typical Kerr rotations obtained from Fe or Co (<21 mdeg). Similar experiment is conducted for single-crystal CoO films grown on MgO(001) substrate [31]. A very interesting trend is observed when the wavelength of the light was varied. The domain contrasts obtained by using the blue light is the strongest one for CoO. The measured energy- dependent MOBE signal may be attributed to the electronic structure of CoO lattice which has a band gap of ~2.8 eV across the Fermi surface. This may cause strong energy- dependent photon excitations [see Figure 3]. Additionally, the domain contrasts depend on the ambient temperature and vanish over the Neel point which is 293K for bulk CoO (and 525K for bulk NiO). The film-thickness dependent results further confirm the stability of the domains down to 1.5 nm CoO film which follows the finite size effect theory. The AFM Neel vector is modified through the exchange coupling in Fe/CoO bilayer. The observed polarization rotation is quantified for 4.6-nm-thick CoO as around 168 mdeg, which is much larger than the NiO film with same thickness.

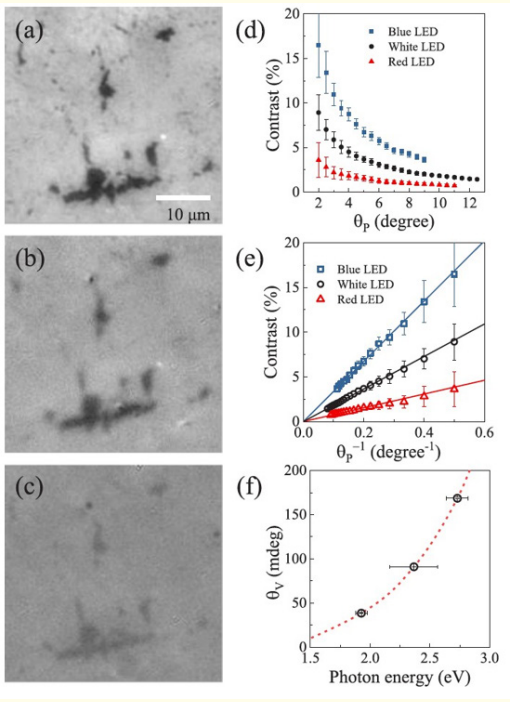

Figure 3: (a)–(c) The optical birefringence images from a 4.6 nm CoO layer measured at 77 K with different LED sources: (a) blue LED, (b) white LED and (c) red LED. (d) and (e) The birefringence asymmetry Iasy as a function of (d) θ_p and (e) θ_{p-1} for different LED sources. (f) The determined polarization rotation angle θv as a function of photon energy. The dashed line is a guide to eyes. Reproduced from Ref. 31 (open source).

Electrical writing and optical reading of AFM domains

In this section the recent developments on unambiguous determination of Neel vector switching by using MOBE microscopy technique is discussed. It resolved the conflicting results which fumed debates about the validity of all-electrical read-write methods, to a great extent. The only solution could be a one-to-one mapping of the electrical response and the optical response before and after altering the magnetic states on the same device. This experiment is reported by Schreiber., *et al*. By combining the MOBE technique with magneto-transport measurement facility, electrical writing and optical reading of the AFM domains are demonstrated [32]. To study the current-induced switching of the insulating NiO, they fabricated NiO(001)(10 nm)/Pt(2 nm) bilayers by epitaxial growth on the MgO(001) substrate. Here, NiO is insulator and Pt conducts current. In an 8- terminal Hall bar (star-shaped) device there are four wide arms for sending write pulses and two narrow arms for read-pulses. The remaining two arms are dedicated for measuring the magnetoresistance signal in terms of transverse voltage change. The sequence is such that, after a ms-long write pulse is applied in one of the easy axis's directions of the NiO lattice, one read pulse of relatively small amplitude is triggered. Transverse voltage is recorded simultaneously. This process is repeated in cycle for both the write arms. After sending five pulses, the directionality of the write pulse is changed. The pristine domain state is largely single domain. It is modified after the application of current density (j_p) close to ~ 10^{12} A/m^2. Thus, sending write pulse in the two orthogonal directions results in a full and reversible commutation between the two magnetic states with dark and bright contrasts. Upon decreasing the current density, the size of the switched area decreases (partial switching). They claimed that this reversible change in contrast can last up to 3 weeks without any relaxation, and is not affected by the external magnetic field of Testa order. The change in write-pulse polarity does not introduce any modification in the outcome as AFM switching is not expected to respond to spin-current polarity (in case there is any contribution from SOT generated in the top Pt layer) unlike ferromagnetic switching. The two important factors, i.e., reproducible switching between the two defined states and their long-term stability are the essential criteria to design nonvolatile spintronics devices. To quantify the

current-induced change, they calculate the difference of initial and final domain images (which is the change in pixel count in a simpler term). The current density is well above the switching threshold. Initially the switched area seems to be quite deviated from the trend followed by the electrical response of the device. After applying many identical pulses, a saturation is reached in the optical response, however the electrical signal increases further with an approximately linear slope. This triangular-shaped electrical signal is observed previously in many all-electrical spin-transport measurements where AFM switching is claimed to occur. Interestingly, coexistence of nonmagnetic contribution along with magnetic response is evidenced in this study. After subtracting the linear slope from the electrical data, a striking similarity is observed in the optical and electrical response from the same device. Now that orthogonal switching of Neel vector is confirmed in AFM heterostructure, it is important to shed light into the underlying mechanisms.

There could be three major contributors: current-induced SOT, current-generated heat, and thermo-magnetoelastic strain. To perform an unequivocal investigation on the existence and weightage of these contributions an NiO(10 nm)/Pt(2 nm) bilayer device is fabricated on MgO(100) substrate similar to the previous studies [33]. The experiment is repeated in similar fashion. According to the SOT mechanism, the final state of the switching depends only on the direction of the current, whereas in the case of the thermo-magnetoelastic switching, it is determined by the distribution and orientation of the temperature gradients in the device due to Joule heating within the metallic layer. The device geometry is depicted in Figure 4. In the first device, the write-arms are patterned deliberately parallel to the easy axis (along [1$\bar{1}$0] and [110]) of NiO lattice. However, for the second device those are fabricated at an angle of 45° to the easy axis (along [100] and [010]). They use Comsol software for simulating the strain generated in the devices. The strain of the NiO lattice due to heat from the straight pulse and X-shaped pulse are opposite. A positive strain difference (represented by red in the original paper) corresponds to a stronger expansion of the NiO along [1$\bar{1}$0] while a negative strain difference (represented by blue in the original paper) corresponds to the orthogonal strain. Though the direction of charge current is same at the center for the device for straight pulse and X-shaped pulse, the strain difference is opposite. This is reflected in the outcome of the experiment as well which is consistent with a thermo-magnetoelastic mechanism that leads to the opposite final states based on the strain. The Joule heating of the NiO layer gives rise to an inhomogeneous expansion

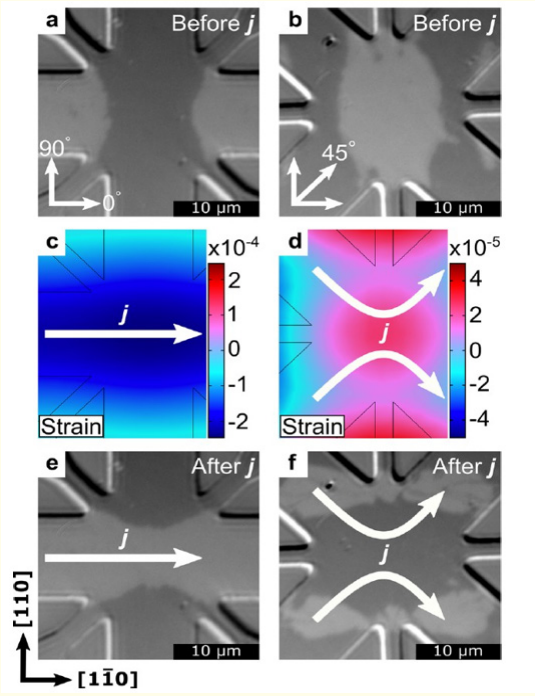

Figure 4: Comparison of the switching between different device geometries. Initial domain structure in the [110] star device (a) and [100] star device (b). Simulations of the current-induced strain ε differences between the easy axes (ε[1$\bar{1}$0]−ε[110]) for a straight pulse along [1$\bar{1}$0] in the [110] star device (c) and for X-shaped pulses along [1$\bar{1}$0] in the [100] star device (d). Domain structure in the [110] star device (e) and [100] star device (f) after applying five pulses in the directions indicated in (c) and (d). We can conclude from the electrical measurements that the dark (light) contrast in the images corresponds to n∥[110] ([1$\bar{1}$0]). Reproduced from Ref. 33 with permission from American Chemical Society.

of the lattice generating stresses compensated by shear strains. This creates a bias to the lattice expansion along the [1$\bar{1}$0] and the [100] directions. Due to lack of degeneracy between the two easy axes, AFM switching occurs!

To further disentangle the contributions from different factors a cross-shaped device with a central dot is designed. It is physically and hence electrically isolated by an annular gap in the Pt layer (See Figure 5). The geometry is so unique that the dot can experience heat and strain, but not the current-induced SOTs from the rest of the device. The magnetization of the NiO layer below the

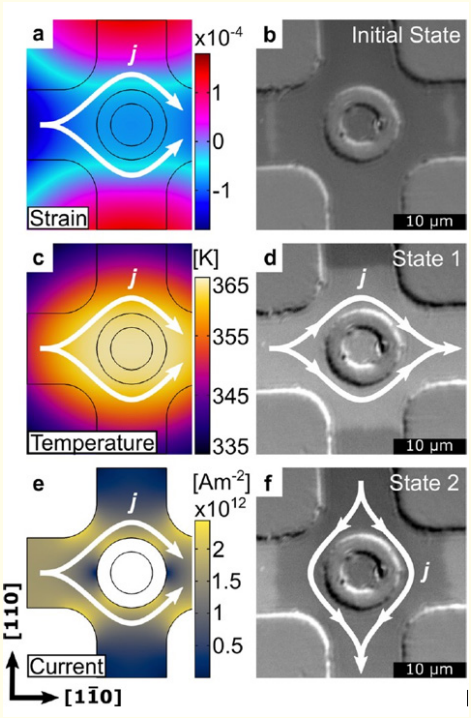

Figure 5: Switching of a device with an electrically isolated area. (a) Simulations of the current-induced strain differences between the easy axis (ε[1$\bar{1}$0]−ε[110]) for a straight pulse along [1$\bar{1}$0] in the cross-shaped device with an inner Pt circle. The corresponding temperature and current profiles are depicted in (c) and (e). The domain structure of the device was imaged before the pulse application along [1$\bar{1}$0] (b) and after (d). Domain structure after a second pulse along [110] (f). Reproduced from Ref. 33 with permission from American Chemical Society.

inner Pt circle can thus be controlled some way or other. The initial domain contrast is presented in Figure 5. After applying write pulse with a current density of 10^{12} A/m^2 there is no partial switching observed. Thus, the requirement of sending multiple pulses is no longer there. The switching is also tested along the [110] direction. A homogeneous switching of NiO underneath the central Pt dot is observed. The current solely is not necessary contributor to the orthogonal switching otherwise an inhomogeneous switching pattern could be formed around the etched ring due to the inhomogeneous current distribution. Thus, the authors conclude that the observed switching is triggered by the combination of Joule heating and strain. It is important to highlight that the strain breaks the degeneracy along the anisotropy axes defining the final state and the assistance from heating helps overcoming the anisotropy barrier at a short instance of time. Furthermore, similar type of switching is observed after inserting MgO spacer layer within the heterostructure and blocking any anticipated spin-current transport from Pt to NiO. This is a confirmation of the fact that SOT is not one of governing mechanisms for Neel-vector switching here.

Till this point it is clear that MOBE microscopy is a powerful optical tool that may speed up the progress of AFM engineering in the near future. Beside using commercial MOKE microscope, it is possible to develop custom-built MOBE microscopy in the laboratory and incorporate equipment as per necessity of the experiments. An upcoming development in this front can be probing of new and exotic AFMs using MOBE technique which has not been done so far. Most of the experimental works in the recent past are limited to NiO heterostructures. The reason might be the possibility of achieving large area switching with high optical contrasts and great reproducibility of the results. However, there are lots of nodes untouched in the material sector which can open Pandora's box. Though the complexity and cost consumption of growing new materials is a matter of concern to the scientists and engineers, recent advancements in oxide-electronics growth techniques will certainly help to cross the hurdles [34]. Another important development could be probing of ultrafast electrical switching of AFMs by synchronizing the pump and optical probe which can pick-up the MOBE signal exhibiting the time dynamics of switching. This will further help the scientific community to truly understand the mechanisms responsible for AFM switching.

Conclusions

In essence, MOBE microscopy is a wide-field, table-top optical imaging technique that facilitate straightforward access to the enigmatic domain configurations in AFMs. Due to having compensated magnetic moments AFM domain contrast is very difficult to probe using any conventional magnetometries. MOBE technique opens up new window to dissect the core of AFM materials. Beside solving the enigma of electrical switching of the Neel vector in the complex AFM heterostructures, this technique is expected to gain more popularity in the scientific community due to its unambiguous installation and interpretation processes.

Acknowledgements

The author would like to acknowledge Shiv Nadar Institution

of Eminence, India and the INSPIRE faculty fellowship scheme sponsored by the Department of Science and Technology, India for providing necessary academic resources during manuscript preparation.

Conflict of Interest

The author declares no conflict of interest.

Bibliography

1. CC Chiang., *et al*. "Absence of evidence of electrical switching of the antiferromagnetic néel vector". *Physical Review Letters* 123 (2019): 1.
2. T Jungwirth., *et al*. "Antiferromagnetic spintronics". *Nature Nanotechnology* 11 (2016): 231.
3. K Olejník., *et al*. "Antiferromagnetic CuMnAs multi-level memory cell with microelectronic compatibility". *Nature Communication* 8 (2017).
4. T Satoh., *et al*. "Spin oscillations in antiferromagnetic NiO Triggered by circularly polarized light". *Physical Review Letters* 105 (2010): 1.
5. SY Bodnar., *et al*. "Writing and reading antiferromagnetic Mn2Au by Néel spin-orbit torques and large anisotropic magnetoresistance". *Nature Communication* 9 (2018): 1.
6. S Nakatsuji., *et al*. *Nature* 527 (2015): 212.
7. W Zhang., *et al*. "Large anomalous Hall effect in a non-collinear antiferromagnet at room temperature". *Physical Review Letters* 113 (2014): 1.
8. P Wadley., *et al*. "Electrical switching of an antiferromagnet". *Science* 351 (2016): 587.
9. J Železný., *et al*. "Relativistic Néel-order fields induced by electrical current in antiferromagnets". *Physical Review Letters* 113 (2014): 1.
10. PH Lin., *et al*. "Manipulating exchange bias by spin-orbit torque". *Nature Material* 18 (2019): 335.
11. XZ Chen., *et al*. "Antidamping-torque-induced switching in biaxial antiferromagnetic insulators". *Physical Review Letters* 120 (2018): 1.
12. T Moriyama., *et al*. *Scientific Report* 8 (2018): 1.
13. L Baldrati., *et al*. "Spin torque control of antiferromagnetic moments in NiO". *Physical Review Letters* 123 (2019): 177201.
14. CG Shull and JS Smart. "Detection of antiferromagnetism by neutron diffraction". *Physical Review* 76 (1949): 1256.
15. SW Cheong., *et al*. "Seeing is believing: visualization of antiferromagnetic domains". *Npj Quantum Material* 5 (2020): 1.
16. M Bode., *et al*. "Atomic spin structure of antiferromagnetic domain walls". *Nature Material* 5 (2006): 477.
17. I Gross., *et al*. *Nature* 549 (2017): 252.
18. U Kaiser., *et al*. "Real-space imaging of non-collinear antiferromagnetic order with a single-spin magnetometer". *Nature* 446 (2007): 522.
19. P Wadley., *et al*. "Current polarity-dependent manipulation of antiferromagnetic domain". *Nature Nanotechnology* 13 (2018): 362.
20. J Stöhr., *et al*. "Images of the antiferromagnetic structure of a NiO (100) surface by means of x-ray magnetic linear dichroism spectromicroscopy". *Physical Review Letters* 83 (1999): 1862.
21. S Mondal and A Barman. "Laser controlled spin dynamics of ferromagnetic thin film from femtosecond to nanosecond timescale". *Physical Review Applied* 10 (2018): 1.
22. T Higo., *et al*. "Large magneto-optical Kerr effect and imaging of magnetic octupole domains in an antiferromagnetic metal". *Nature Photonics* 12 (2018): 73.
23. V Saidl., *et al*. "Optical determination of the Néel vector in a CuMnAs thin-film antiferromagnet". *Nature Photonics* 11 (2017): 91.
24. WL Roth. "Neutron and optical studies of domains in NiO". *Journal of Applied Physics* 31 (1960): 2000.
25. H Matsuyama., *et al*. "Microscopic imaging of Fe magnetic domains exchange coupled with those in a NiO (001) surface". *Physical Review Letters* 85 (2000): 646.
26. JY Chauleau., *et al*. *Nature Material* 16 (2017): 803.

27. I Gray., *et al*. "Multi-stimuli manipulation of antiferromagnetic domains assessed by second-harmonic imaging". *Physical Review X* 9 (2019): 41016.

28. PM Oppeneer. "Lighting up antiferromagnets". *Nature Photonics* 11 (2017): 74.

29. R Schäfer and A Hubert. "A new magnetooptic effect related to non-uniform magnetization on the surface of a ferromagnet". *Physica Status Solidi* 118 (1990): 271.

30. J Xu., *et al*. "Imaging antiferromagnetic domains in nickel oxide thin films by optical birefringence effect". *Physical Review B* 100 (2019): 134413.

31. J Xu., *et al*. "Optical imaging of antiferromagnetic domains in ultrathin CoO (001) films". *New Journal of Physics* 22 (2020).

32. F Schreiber., *et al*. "Concurrent magneto-optical imaging and magneto-transport readout of electrical switching of insulating antiferromagnetic thin films". *Applied Physics Letters* 117 (2020).

33. H Meer., *et al*. "Direct imaging of current-induced antiferromagnetic switching revealing a pure thermomagnetoelastic switching mechanism in NiO". *Nano Letter* 21 (2021): 114.

34. P Němec., *et al*. "Efficient spin excitation via ultrafast damping-like torques in antiferromagnets". *Nature Physics* 14 (2018): 229.